Effect of V-doping on the electronic structure of $Bi_2Zr_2O_7$: A first-principles study

Shigenori Matsushima, Ryo Kaminaga, Junko Ishii, Masao Arai*, Kenji Obata

Abstract

In the present study, a first-principles energy band calculation is performed for the V-doped $Bi_2Zr_2O_7$ (V-doped BZO) supercell and pure BZO unit cell to elucidate the effect of V doping on the electronic structure and optical properties. Structural optimization calculation reveals that the theoretical lattice constant of the BZO unit cell almost agrees with the experimental value. The minimum bandgap is estimated to be 2.55 eV. The density-of-states (DOS) calculation indicates that the valence band (VB) located is mainly composed of O 2*p* states and mixed with Bi 6p and Zr 4*d* states throughout the VB. Alternatively, the conduction band (CB) is mainly composed of Zr 4*d* states and is mixed with the O 2*p* and Bi 6*p* states. When the BZO is doped with a V atom, three strongly localized peaks appear in the bandgap of the BZO and are assigned to the V 3*d* states. Based on the dielectric function calculation of the V-doped BZO cell, there are absorption peaks from the O 2*p* VB states to the V 3*d* gap states and a VB–CB optical transition in the BZO crystal. In addition, these peaks are confirmed on the absorption coefficient curves and can be attributed to the charge-transfer absorption from O 2*p* VB states to V 3*d* gap states. Therefore, the optical absorption of BZO in the visible light region is expected to be enhanced by the addition of the V atom.

Keywords: *$Bi_2Zr_2O_7$, V-doped $Bi_2Zr_2O_7$, Ab initio calculation, Electronic structure, Optical properties*

1. Introduction

Recently, there is a growing concern that elements have a harmful effect on human health and the natural environment. Thus, environment-friendly metal oxides consisting Zn, Zr, Ce, La, and Bi are proposed as a new ceramic pigment material, instead of toxic metallic elements such as Cr, Cd, Sb, and Pb. Among the ceramic pigments, yellow color is in high demand owing to its high visibility [1]. Vanadium is a typical dopant for yellowing oxides with a wide bandgap, and vanadium zirconia yellow (V-doped ZrO_2) and vanadium tin yellow (V-doped SnO_2) have been developed to date [2-7]. However, yellow color is not sufficient owing to the small amount of V dissolved in the host oxide. Therefore, it is often used mixed with praseodymium yellow (Pr-doped $ZrSiO_4$), which has a bright yellow color [8, 9], but it should be remembered that Pr is a rare element. Accordingly, the development of new yellow ceramic pigments is awaited. When introducing the dopant into the host ceramics, the ionic radius ratio between the dopant element and host crystal is an important factor controlling the solubility limits of the dopant element. The pyrochlore-type structure is expressed in $A_2B_2O_7$ and the eightfold coordinated A-site, and octahedral B-site can be occupied by various cations having a wide range of ionic radii [10]. This fact suggests that the pyrochlore oxides are a promising matrix for developing a new ceramic pigment material.

In this study, we focus on $Bi_2Zr_2O_7$ (BZO) with a pyrochlore-type structure and perform first-principles calculations to acquire detailed information regarding the effect of adding a V atom with tetra valence state (V^{4+}). In particular, we have explored the characteristics of the valence band (VB) and conduction band (CB) as well as the optical properties of the V-doped BZO supercell.

2. Calculation method

The BZO unit cell was optimized by relaxing all the lattice constants and atomic positions using the Cambridge Serial Total Energy Package (CASTEP) code [11]. All the optimization calculations were performed using the Broyden–Fletcher–Goldfarb–Shanno algorithm [12]. Exchange and correlation interactions were treated within the framework of a generalized gradient approximation (GGA) proposed by Perdew *et al* [13]. Cutoff energy of the plane-wave expansions was set to 380 eV, and the valence electrons are treated with Vanderbilt-type non-local ultra-soft pseudopotentials [14]. Reciprocal-space integration in the first Brillouin zone (FBZ) is performed using four irreducible k-points, which correspond to a 2 × 2 × 2 k-grid of the Monkhorst-Pack scheme [15]. A V-doped BZO supercell was constructed by substituting a V atom for a Zr atom in the BZO unit cell, as shown in **Fig. 1**. The supercell was optimized by relaxing all atomic positions using the CASTEP code. The lattice constant, *a*, was assumed to have the same values as those in the BZO unit cell. Each self-consistency was examined based on the convergence criteria, which were the energy change per atom (5.0×10^{-6} eV/atom), the atomic displacement (5.0×10^{-4} Å), the force on the atoms (1.0×10^{-2} eV/Å), and the stress on the atoms (2.0×10^{-2} GPa).

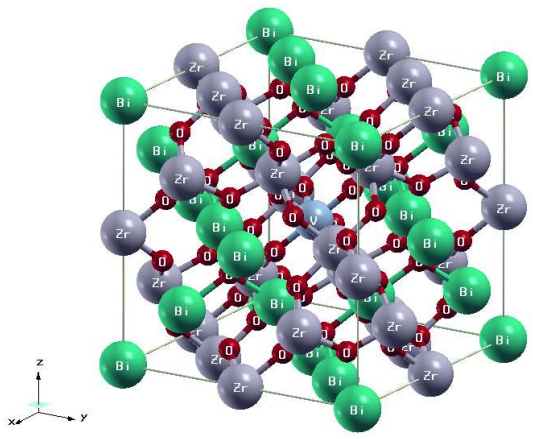

Fig. 1 V-doped $Bi_2Zr_2O_7$ supercell.

*National Institute for Materials Science (NIMS)

The electronic structure calculations of the V-doped BZO supercell and pure BZO unit cell were performed using the scalar-relativistic full-potential linearized augmented plane-wave (FLAPW + *lo*) method based on the GGA approach [16]. The wave functions were expanded using the augmented plane-wave basis functions comprising of plane-waves in the interstitial region and linear combinations of radial functions multiplied by spherical harmonics inside the muffin-tin (MT) region. The MT spheres radii (R_{MT}) of the Bi, Zr, and O atoms were 2.32, 2.02, and 1.70 a.u., respectively, for the BZO unit cell, and that of the V, Bi, Zr, and O atoms were 1.88, 2.31, 2.02, and 1.70 atoms, respectively, for the V-doped BZO supercell. The plane-wave cutoff was $R_{MT}*K_{max} = 7.0$ for both cells. The Brillouin-zone (BZ) integrations were conducted via a modified tetrahedron method using a 10 × 10 × 10 *k*-mesh (47 *k*-points) for the BZO unit cell and using a 4 × 4 × 4 *k*-mesh (32 *k*-points) for the V-doped BZO supercell in a first BZ.

The optical properties of V-doped BZO supercell and BZO unit cell were derived using the complex dielectric function, $\varepsilon(\omega) = \varepsilon_1(\omega) + i\varepsilon_2(\omega)$ [17]. The imaginary part of the dielectric function, $\varepsilon_2(\omega)$ was numerically calculated using the momentum matrix elements between the unoccupied and occupied electronic states based on the selection rules, whereas the real part, $\varepsilon_1(\omega)$ was converted using $\varepsilon_2(\omega)$ by the Kramers–Kronig relation. These properties were broadened by Lorentzian functions with γ = 0.10 eV. Furthermore, the absorption coefficient $I(\omega)$ was estimated using the complex dielectric function $\varepsilon(\omega)$. The absorption coefficient is given by the following equation [17, 18]:

$$I(\omega) = \left(\sqrt{2}\omega/c\right)\left[\sqrt{\varepsilon_1(\omega)^2 + \varepsilon_2(\omega)^2} - \varepsilon_1(\omega)\right]^{1/2} \quad (1)$$

where c denotes the velocity of light in a vacuum.

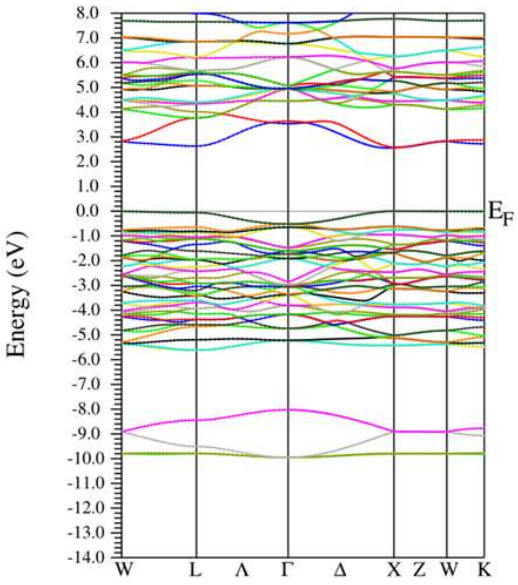

Fig. 2 Energy band structure of $Bi_2Zr_2O_7$.

3. Results and discussion

Pyrochlore-type structure with the general formula $A_2B_2O_7$ crystallizes into a cubic system with space group *Fd-3m* and contains eight formula units for 88 atoms as shown (**Fig. 1**). In this structure, there is one independent A atom, one independent B atom, and two independent O atoms (O1 and O2). A and B atoms occupy the Wyckoff 16*c* position. O1 and O2 atoms occupy the Wyckoff 48*f* and 8*a* positions, respectively. In the case of BZO crystals, the Bi 6s electron pair is strongly localized on the Bi atom, causing steric hindrances for the arrangement of ions. The hindrances can result in the displacement of the Bi atoms from ideal positions to the positions Wyckoff 96*h*, 96*g*, or 192*i*, and consequently, in the displacements of the O2 atoms [19, 20]. In this calculation, we have assumed that BZO has an ideal pyrochlore-type structure for simplifying the calculations for impurity-doped supercells. The optimization calculation was conducted for the ground state of the system at 0 Pa and 0 K. The lattice constant and atomic positions remained almost unchanged compared with the experimental data after the optimization [19].

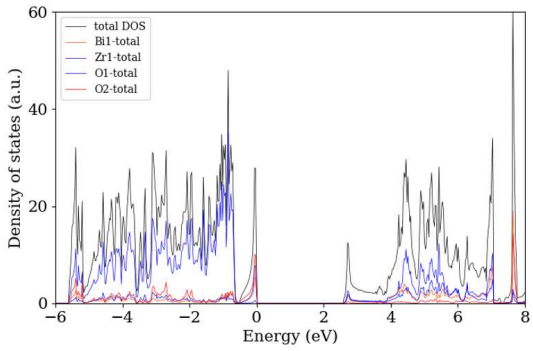

Fig. 3 DOS of $Bi_2Zr_2O_7$ unit cell.

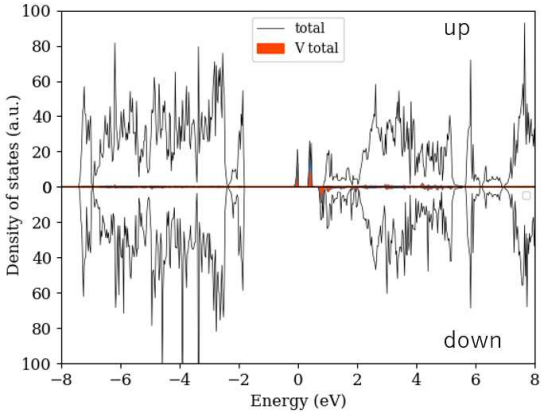

Fig. 4 DOS of V-doped $Bi_2Zr_2O_7$ supercell.

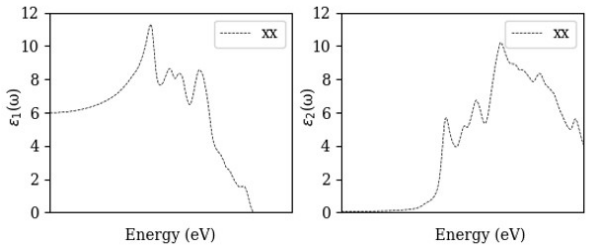

Fig. 5 $\varepsilon_1(0)$ and $\varepsilon_2(\omega)$ of the theoretical dielectric function of the $Bi_2Zr_2O_7$ unit cell.

Figure 2 shows the energy band structure along with high-symmetry directions of the first BZ for the optimized BZO unit cell. The origin of energy (Fermi level) is taken at the valence band maximum (VBM). W, L, Γ, X, and K are symmetry points, whose coordinates are (1.0, 0.5, 0), (0.5, 0.5, 0.5), (0, 0, 0), (1.0, 0.5, 0), and (0.75, 0.75, 0), respectively, in units of g_1^*, g_2^*, and g_3^* (g_1^*, g_2^*, and g_3^* are the relevant reciprocal-space vectors). The minimum band gap was calculated to be 2.55 eV, which is close to the approximate experimental values reported in the literatures [21-23]. The VBM and conduction band minimum (CBM) are both located near the X point, but slightly different, suggesting that BZO is an indirect material. However, it is uncertain whether BZO is a direct-gap or an indirect-gap material owing to the very small energy difference between the direct and indirect transitions.

Figure 3 shows the total density-of-states (TDOS) and partial density-of-states (PDOS) for the Bi, Zr, O1, and O2 atoms of the BZO unit cell. From the comparison of the TDOS and PDOS, the VB located from −5.61 to 0 eV can be observed to be mainly composed of O 2*p* states and mixed with Bi 6*p* and Zr 4*d* states throughout the VB. The nearest atoms of O1 are Zr, and the ones of O2 are Bi. Therefore, the DOS of O1 and O2 significantly differ in shape. The Bi 6s states are strongly localized near the top of the valence band, which corresponds to the classically known inactive electron pair of Bi 6s [24]. Alternatively, the CB mainly comprises Zr 4d states, and it is mixed with the O 2*p* and Bi 6*p* states.

Figure 4 (a) shows the TDOS and V-related DOS for the V-doped BZO supercell. When BZO is doped with a V atom, sharp localized peaks that were not identified before doping are observed in the bandgap of BZO. In the up-spin states, the lowest gap states are located at E = 0 eV, indicating that the V-doped BZO is metallic. The energy difference from the VBM of BZO is estimated to be *ca.* 1.82 eV. According to the PDOS analysis, the localized peaks were found to be mainly in the V 3*d* states and are also hybridized with the O 2*p* states. Three peaks form in the bandgap lie in the range of –0.11 to 0 eV (Peak-I), 0.35 to 0.42 eV (Peak-II), and 0.42 to 0.46 eV (Peak-III), but Peak-II and Peak-III are very close. Peak-I is mainly attributable to V $3d_{xy}$, $3d_{xz}$, and $3d_{yz}$ states, whereas Peak-II and Peak-III are mainly attributable to V $3d_{x^2-y^2}$ and V $3d_{z^2}$ states, respectively. This result is explained by deformation of the

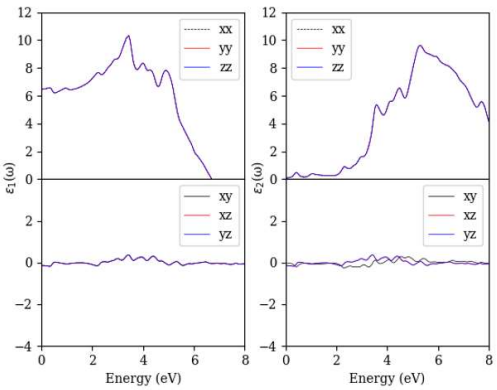

Fig. 6 $\varepsilon_1(0)$ and $\varepsilon_2(\omega)$ of the theoretical dielectric function of the V-doped $Bi_2Zr_2O_7$ supercell.

VO6 octahedron in the V-doped BZO supercell, as presented in Table 1. In the down-spin states, there are two peaks in the range of 0.71 to 0.82 eV (Peak-IV) and 0.82 to 0.90 eV (Peak-V). Peak-IV and Peak-V are mainly attributable to V $3d_{x^2-y^2}$ and V $3d_{z^2}$ states, respectively, and V $3d_{xy}$, $3d_{xz}$, and $3d_{yz}$ states make little contribution.

Figure 5 depicts the real $\varepsilon_1(\omega)$ and imaginary $\varepsilon_2(\omega)$ parts of the dielectric function for the BZO unit cell. The dielectric tensor contains one independent diagonal component, ε_{xx}, because BZO has a cubic crystal system. The real part $\varepsilon_1(0)$is equal to the square of the refractive index, *i.e.*, approximately 2.45. The imaginary part $\varepsilon_2(\omega)$ is related to the absorption spectrum between the electronic transitions from VB to CB and shows the maximum value at 3.5 eV. This peak is mainly attributed to the electronic transition from Bi 6s and O 2p to Bi 6p and O 2p, as shown in **Fig. 4**.

Figure 6 denotes $\varepsilon_1(\omega)$ and $\varepsilon_2(\omega)$ of the dielectric function for the V-doped BZO supercell. Owing to the triclinic structure of V-doped BZO supercell, $\varepsilon_1(\omega)$ and $\varepsilon_2(\omega)$ can be separated into six independent components, which are three diagonal components (*xx*, *yy*, *zz*) and three off-diagonal components (*xy*, *xz*, *yz*). However, the three diagonal components overlap each other and appear to be a single curve, as well as for the three non-diagonal components. The refractive index $\varepsilon_1(0)$of the supercell is larger than the value of pure BZO. On the contrary, in the $\varepsilon_2(\omega)$, several small peaks were found at 0.42, 1.05, 2.33 eV, and so on.

Moreover, the absorption coefficient $I(\omega)$ for V-doped BZO supercell and BZO unit cell are calculated, and those results are shown in **Fig. 7**. Because the coefficients are derived using the dielectric function, each polarization tensor component is similar to the corresponding components of the dielectric function. In **Fig. 7**, there are several peaks at 0.45, 1.07, 2.35 eV, and so on in the V-doped BZO supercell, as indicated by **Fig. 6**. These peaks can be attributed to the charge-transfer absorption from O 2*p* VB to V 3*d* gap states and the dd transition between V 3*d* states. Needless to say, these peaks do not appear without V addition. Therefore, the addition of V into BZO crystal is expected to improve the optical

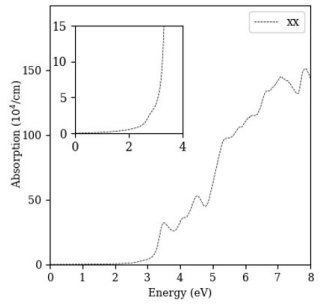

(a)

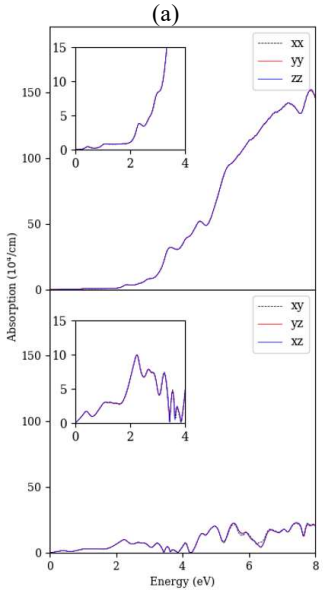

(b)

Fig. 7 Absorption coefficient, *I*, for the (a) $Bi_2Zr_2O_7$ unit cell and (b) V-doped $Bi_2Zr_2O_7$ supercell.

absorption of BZO in the visible light region.

4. Conclusion

We performed a first-principles energy band calculation for the V-doped BZO supercell and pure BZO unit cell using the theoretically optimized structure to elucidate the effect of V doping on the electronic structure and optical properties. The minimum bandgap of the BZO is estimated to be 2.55 eV. The DOS analysis reveals that VB is mainly composed of O 2*p* states and mixed with Bi 6*p* and Zr 4*d* states, and the CB is mainly composed of Zr 3*d* states mixed with the O 2*p* and Bi 6*p* states. In the dielectric function calculation of the V-doped BZO supercell, small absorption peaks are observed from the O 2*p* VB to the V 3*d* gap states as well as the VB–CB optical transition in the BZO crystal. These peaks can be confirmed on the absorption coefficient curves and are attributed to charge-transfer absorption from O 2*p* VB to V 3*d* gap states.

References

[1] T. Masui, Wendusu, N. Imanaka, J. Jpn. Soc. Color Mater., **84**, 439-443 (2011) [in Japanese].

[2] F. Ren, S. Ishida, N. Takeuchi, J. Am. Ceram. Soc., **76**, 1825-1831 (1993).

[3] K. Fujiyoshi, H. Yokoyama, F. Ren, S. Ishida, J. Am. Ceram. Soc., **76**, 981-986 (1993).

[4] R.G. Egdell, A. Gulino, C. Rayden, G. Peacock, P.A. Cox, J. Mater, Sci., **5**, 499-504 (1995).

[5] P. Zhang, G. Wu, X. Chi, Y. Wang, S. Liu, Inorg. Mater., **42**, 681-683 (2006).

[6] C. Dziubak, Mater. Sci. Poland, 30, 398-405 (2012).

[7] Z. Hu, Q. Wang, J. Liu, K. Liu, W. Zhang, Y. Yang, Y, Wang, Q. Chang, J. Alloys Compd., **856**, 157397 (2021).

[8] G.D. Nero, G. Cappeletti, S. Ardizzone, P. Fermo, S. Gilardoni, J. Eur. Ceram. Soc., **24**, 3603-3611 (2004).

[9] H.H. Rivera-Yerena, J.F. Louvier-Hernández, F.J. Garcíia-Rodriguez, L.S. Medrano, E. Pérez, R. Patiño-Herrera, J. Solid State Chem., **297**, 122084 (2021).

[10] S. Ishida, F. Ren, N. Takeuchi, J. Am. Ceram. Soc., **76**, 2644-2648 (1993).

[11] V. Milman, B. Winkler, J. A. White, C. J. Pickard, M. C. Payne, E. V. Akhmatskaya, R.H. Nobes, Int. J. Quantum Chem., **77**, 895-910 (2000).

[12] B.G. Pfrommer, M. Câté, S.G. Louie, M.L. Cohen, J. Comput. Phys., **131**, 233-240 (1997).

[13] J.P. Perdew, K. Burke, M. Ernzerhof, Phys. Rev. Lett., **77**, 3865-3868 (1996).

[14] D. Vanderbilt, Phys. Rev. B, **41**, 7892-7895 (1990).

[15] H.J. Monkhorst, J.D. Pack, Phys. Rev. B, **13**, 5188-5192 (1976).

[16] P. Blaha, K. Schwarz, G.K.H. Madsen, D. Kvasnicka, J. Luitz, "WIEN2k, An Augmented Plane Wave + Local Orbitals Program for Calculating Crystal Properties", K. Schwarz, Techn. Universitat Wien, Austria (2001), ISBN 3-9501031-1-2.

[17] C. Ambrosch-Draxl, J. Sofo, Comput. Phys. Commun., **175**, 1-14 (2006).

[18] H. Salehi, H. Tolabinejad, Opt. Photonics J, **1**, 75-80 (2011).

[19] A.L. Hector, S.B. Wiggin, J. Solid State Chem., **177**, 139-145 (2004).

[20] J.R. Esquivel-Elizondo, B.B. Hinojosa, J.C. Nino, Chem. Mater., **23**, 4965-4974 (2011).

[21] V.M. Shama, D. Saha, G. Madras, T.N.G. Row, RSC Adv., **3**, 18938-18943 (2013).

[22] D. Wu, T. He, J. Xia, Y. Tan, Mater. Lett., **156**, 195-197 (2015).

[23] Y. Luo, L. Cao, L. Feng, J. Huang, L. Yang, C. Yao, Y. Cheng, Mater. Sci. Eng. B, **240**, 133-139 (2019).

[24] Y. Obukuro, S. Matsushima, K. Obata, M. Arai, K. Kobayashi, J. Phys. Chem. Solids, **75**, 427-432 (2014).